

The Informed Elastic Net for Fast Grouped Variable Selection and FDR Control in Genomics Research

Jasin Machkour

Technische Universität Darmstadt
64283 Darmstadt, Germany
jasin.machkour@tu-darmstadt.de

Michael Muma

Technische Universität Darmstadt
64283 Darmstadt, Germany
michael.muma@tu-darmstadt.de

Daniel P. Palomar

The Hong Kong University of Science and Technology
Clear Water Bay, Hong Kong SAR, China
palomar@ust.hk

Abstract—Modern genomics research relies on genome-wide association studies (GWAS) to identify the few genetic variants among potentially millions that are associated with diseases of interest. Only reproducible discoveries of groups of associations improve our understanding of complex polygenic diseases and enable the development of new drugs and personalized medicine. Thus, fast multivariate variable selection methods that have a high true positive rate (TPR) while controlling the false discovery rate (FDR) are crucial. Recently, the T-Rex+GVS selector, a version of the T-Rex selector that uses the elastic net (EN) as a base selector to perform grouped variable election, was proposed. Although it significantly increased the TPR in simulated GWAS compared to the original T-Rex, its comparably high computational cost limits scalability. Therefore, we propose the informed elastic net (IEN), a new base selector that significantly reduces computation time while retaining the grouped variable selection property. We quantify its grouping effect and derive its formulation as a Lasso-type optimization problem, which is solved efficiently within the T-Rex framework by the terminated LARS algorithm. Numerical simulations and a GWAS study demonstrate that the proposed T-Rex+GVS (IEN) exhibits the desired grouping effect, reduces computation time, and achieves the same TPR as T-Rex+GVS (EN) but with lower FDR, which makes it a promising method for large-scale GWAS.

Index Terms—Informed elastic net, T-Rex selector, grouped high-dimensional variable selection, FDR control, GWAS.

I. INTRODUCTION

Fast grouped variable selection is essential in many modern signal processing applications such as genomics research [1], direction-of-arrival (DOA) estimation [2], and financial index tracking [3], where groups of highly correlated variables are present in the data [4]–[6]. In this paper, we focus on modern genomics research that aims at understanding complex genetic diseases in order to enable personalized medicine and the development of new drugs. In genomics research, a useful and widespread tool for the discovery of the few single nucleotide polymorphisms (SNPs) (among potentially millions of SNPs) that are associated with a disease of interest are genome-wide association studies (GWAS) [1]. More specifically, in GWAS the aim is to detect as many as possible of the SNPs that are associated with a disease of interest while keeping the number of false discoveries low. Thus, false discovery rate (FDR)-controlling variable selection methods that exhibit a high true positive rate (TPR) are required. The FDR is defined as the expected fraction of false discoveries among all discoveries, i.e., $\text{FDR} = \mathbb{E}[\# \text{ False discoveries} / \# \text{ Discoveries}]$, while the TPR is defined as the expected fraction of true discoveries among all true active variables, i.e., $\text{TPR} = \mathbb{E}[\# \text{ True discoveries} / \# \text{ True actives}]$. However, since the

number of SNPs p (i.e., variables) usually exceeds the number of subjects n (i.e., samples), the existing FDR-controlling methods for the low-dimensional setting [7]–[10] are not applicable in this high-dimensional setting (i.e., $p > n$). In recent years, two multivariate FDR-controlling variable selection frameworks for the high-dimensional setting have been proposed: the *T-Rex* selector [11] and the *model-X* knockoff method [12]. Among these two frameworks, only the *T-Rex* selector is scalable to millions of variables and, therefore, applicable for real world high-dimensional GWAS with millions of variables in a reasonable computation time (see Figure 1 in [11], and [13]). Recently, the *T-Rex+GVS* selector was proposed [14]. It is an extension of the *T-Rex* selector that uses the elastic net [15] as a base selector to perform grouped variable selection and, thereby, significantly increases the TPR compared to the original *T-Rex* selector in grouped variable selection problems. Unfortunately, however, this performance increase came at the cost of an increased computation time, which (in practice) reduces its scalability to very large GWAS.

Original Contributions: We propose the *informed elastic net (IEN)*, a new base selector that performs grouped variable selection while significantly reducing the computation time compared to the original *elastic net (EN)*. We prove that the proposed *IEN*

- 1) can be formulated as a *Lasso*-type optimization problem (Theorem 1) and, therefore, can be solved efficiently in a forward-selection manner, as required by the *T-Rex* framework, using the *LARS* algorithm [16] and
- 2) exhibits a grouping effect (Theorem 2) that is similar to that of the elastic net.

Additionally, we validate empirically that the proposed *IEN*, as suggested by Theorems 1 and 2,

- 1) produces solution paths that are similar to the ones of the *EN* (see Figure 2),
- 2) significantly reduces the computation time compared to the *EN* when incorporated into the *T-Rex* framework as the base selector (see Figure 3), and
- 3) has the same TPR as the *T-Rex+GVS* selector using the *EN* while achieving a much lower FDR in a simulated GWAS (see Figure 4).

An open source implementation of the proposed method is available in the R package *TRexSelector* on CRAN [17].

Organization: Section II briefly revisits the existing *T-Rex* framework. In Section III, the proposed *informed elastic net (IEN)* is presented. Section IV compares the proposed *informed elastic net* against the elastic net in terms of performance and computation time, while Section V presents the results of a simulated GWAS, in which the proposed *IEN* is used as the base selector within the *T-Rex* framework. Section VI concludes the paper and the proofs of Theorems 1 and 2 are deferred to the appendix.

The first and second author are supported by the LOEWE initiative (Hesse, Germany) within the emergenCITY center. The second author is also supported by the ERC Starting Grant ScReeningData. The third author is supported by the Hong Kong GRF 16207820 research grant.

Extensive calculations on the Lichtenberg High-Performance Computer of the Technische Universität Darmstadt were conducted for this research.

II. THE T-REX+GVS SELECTOR

This work builds upon the Terminating-Random Experiments (*T-Rex*) selector [11], a recently developed variable selection framework for high-dimensional data that controls any user-defined target FDR (Theorem 1 in [11]) while maximizing the number of selected variables. This is achieved by mathematically modeling and fusing the solutions of K early terminated random experiments, where computer-generated dummy variables compete with real variables. Figure 1 shows a schematic overview of the *T-Rex* selector. The main steps are briefly revisited in the following. First, K dummy matrices $\tilde{\mathbf{X}}_k \in \mathbb{R}^{n \times L}$, $k = 1, \dots, K$, are generated (each containing L dummy predictor vectors). The elements of the dummy predictors can be generated from any univariate probability distribution with finite mean and variance, e.g., the standard normal distribution (Theorem 2 in [11]). Second, the dummy matrices are appended to the original predictor matrix $\mathbf{X} = [\mathbf{x}_1 \cdots \mathbf{x}_p] \in \mathbb{R}^{n \times p}$ to obtain the extended predictor matrices $\tilde{\mathbf{X}}_k = [\mathbf{X} \ \tilde{\mathbf{X}}_k]$, $k = 1, \dots, K$. Third, early terminated random experiments are conducted by feeding $\tilde{\mathbf{X}}_k$, $k = 1, \dots, K$, and \mathbf{y} into a base forward variable selection algorithm, such as the *LARS* algorithm [16] or the *Lasso* [18], and terminating each selection process after T dummies have been included. The obtained candidate variable sets $\mathcal{C}_{k,L}(T)$, $k = 1, \dots, K$, are fused to obtain the relative occurrences of the original variables $\Phi_{T,L}(j)$, $j = 1, \dots, p$. The final selected active set contains all variables whose relative occurrences exceed a voting threshold $v \in [0.5, 1)$, i.e., $\hat{\mathcal{A}}_L(v^*, T^*) := \{j : \Phi_{T^*,L}(j) > v^*\}$. The extended calibration algorithm automatically chooses the values of L , T^* , and v^* , such that the FDR is controlled at the target level $\alpha \in [0, 1]$, while maximizing the number of selected variables.

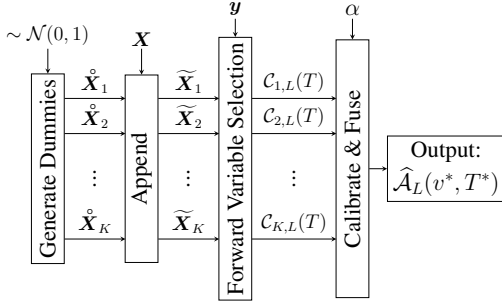


Figure 1: Sketch of the *T-Rex* selector framework [11], [14].

The *T-Rex+GVS* selector, where *GVS* stands for grouped variable selection, was proposed recently as an extension of the *T-Rex* selector [14]. It was proven that, when incorporating the elastic net as the base forward variable selector into the *T-Rex* framework, the grouped variable selection property of the elastic net, whose solution is defined by

$$\hat{\beta}_{\text{EN}} := \arg \min_{\beta} \|\mathbf{y} - \mathbf{X}\beta\|_2^2 + \lambda_1 \|\beta\|_1 + \lambda_2 \|\beta\|_2^2, \quad (1)$$

where $\lambda_1, \lambda_2 > 0$, carries over to the *T-Rex+GVS* selector [14]. Note that when incorporating the elastic net into the *T-Rex* framework, the sparsity parameter λ_1 is automatically determined according to the user-defined target FDR level and does not require any tedious and computationally expensive tuning. The parameter λ_2 is chosen as suggested in [14] via a cross validation of Ridge regression solutions.

Moreover, for grouped variables, such as in GWAS, it was shown that using the *elastic net* as the base selector within the

T-Rex framework leads to a significant increase in the TPR, while controlling the FDR at the user-defined target level.

III. PROPOSED: THE INFORMED ELASTIC NET (IEN)

While the *EN* achieves its grouping effect by penalizing $\|\beta\|_2^2$, this section presents a new *GVS* method that incorporates the information of how the variables are grouped into its penalty term. We show that the proposed *IEN* can be formulated as a *Lasso*-type optimization problem (Theorem 1), so that it can be incorporated into the *T-Rex* framework. We also analyze the grouping effect (Theorem 2) and show that the *IEN* boils down to the *EN* when every variable is considered to be its own group (Corollary 1).

In particular, the proposed *IEN* uses single-linkage hierarchical clustering [19] with the pairwise correlations of the original variables as a distance measure to cluster variables into groups of highly correlated variables, which are present in genomics data due to a phenomenon called linkage disequilibrium [4]. The obtained dendrogram from the hierarchical clustering can be cut at different levels to obtain M disjoint groups of variables $\mathcal{G}_1, \dots, \mathcal{G}_M$, where $M \leq p$. To represent the m th, $m = 1, \dots, M$, group mathematically, we define the binary support vector $\mathbf{1}_m = [1_{m,1} \cdots 1_{m,p}]^T \in \{0, 1\}^p$ that has one entries for variables in the m th group and zero entries otherwise. The corresponding group size is $p_m := \sum_{j=1}^p 1_{m,j}$. With these definitions in place, we define the proposed *IEN*.

Definition 1 (*Informed elastic net (IEN)*). Let $\lambda_1, \lambda_2 > 0$ and let p_m , $m = 1, \dots, M$, and $\mathbf{1}_m \in \{0, 1\}^p$ be the known group size and the binary support vector of the m th group, respectively. Then, the Lagrangian of the informed elastic net (*IEN*) is defined by

$$\mathcal{L}_{\text{IEN}}(\beta) := \|\mathbf{y} - \mathbf{X}\beta\|_2^2 + \lambda_1 \|\beta\|_1 + \lambda_2 \sum_{m=1}^M \frac{(\mathbf{1}_m^\top \beta)^2}{p_m} \quad (2)$$

and the solution of the *IEN* is defined by

$$\hat{\beta} := \arg \min_{\beta} \mathcal{L}_{\text{IEN}}(\beta). \quad (3)$$

The following theorem shows that the proposed *IEN* can be cast as a *Lasso*-type optimization problem and, therefore, can be solved efficiently and in a forward selection fashion, as required by the *T-Rex* framework, using the *LARS* algorithm:¹

Theorem 1 (*Lasso-type optimization problem*). Let \mathbf{X} , \mathbf{y} , and $\lambda_1, \lambda_2 > 0$ be given and let $\mathbf{0}_M$ be the M -dimensional vector of zeros. Define

$$\mathbf{X}' := \sqrt{\lambda_2} \cdot \begin{bmatrix} \mathbf{X}/\sqrt{\lambda_2} \\ \mathbf{1}_1^\top/\sqrt{p_1} \\ \vdots \\ \mathbf{1}_M^\top/\sqrt{p_M} \end{bmatrix}, \quad \mathbf{y}' := \begin{bmatrix} \mathbf{y} \\ \mathbf{0}_M \end{bmatrix}. \quad (4)$$

Then, the *IEN* can be formulated as a *Lasso*-type optimization problem, i.e.,

$$\mathcal{L}_{\text{IEN}}(\beta) = \|\mathbf{y}' - \mathbf{X}'\beta\|_2^2 + \lambda_1 \|\beta\|_1. \quad (5)$$

Remark 1. Note that, in contrast to the *EN*, the *IEN* data augmentation presented in Theorem 1 requires appending only M additional rows to the original predictor matrix \mathbf{X} , while

¹Note that the proposed *IEN* is fundamentally different from the *group Lasso* approach in [20], since the solution path of the *group Lasso* is not piecewise linear and, therefore, computationally much more expensive.

solving the elastic net in a forward selection manner requires appending p rows to \mathbf{X} (for details, see [15]). Since the number of variable groups M , especially in genomics data, is much smaller than the number of variables p (i.e., $M \ll p$), the IEN exhibits a significantly reduced computation time when p is very large.

The next theorem shows that the proposed *informed elastic net* exhibits a grouping effect, i.e., the difference of the averaged coefficients of any two variable groups is shrunk towards zero according to the maximum correlation between two variables from different groups:

Theorem 2 (IEN grouping effect). Define $\rho_{j,j'} := \mathbf{x}_j^\top \mathbf{x}_{j'}$, where \mathbf{x}_j and $\mathbf{x}_{j'}$ are standardized predictors. Suppose that $\hat{\beta}_j \hat{\beta}_{j'} > 0$ and, without loss of generality, $j \in \mathcal{G}_1$ and $j' \in \mathcal{G}_2$. Then, it holds that

$$\begin{aligned} & \frac{1}{\|\mathbf{y}\|_2} \left| \frac{1}{p_1} \sum_{g \in \mathcal{G}_1} \hat{\beta}_g - \frac{1}{p_2} \sum_{g \in \mathcal{G}_2} \hat{\beta}_g \right| \\ &= \frac{1}{\|\mathbf{y}\|_2} \left| \frac{\mathbf{1}_1^\top \hat{\boldsymbol{\beta}}}{p_1} - \frac{\mathbf{1}_2^\top \hat{\boldsymbol{\beta}}}{p_2} \right| \leq \frac{1}{\lambda_2} \sqrt{2 \left(1 - \max_{j \in \mathcal{G}_1, j' \in \mathcal{G}_2} \{\rho_{j,j'}\} \right)}. \end{aligned}$$

Corollary 1. The grouping effect of the proposed IEN is identical to that of the EN, when every variable is considered to be a group.

Proof. When every variable is considered to be a group, we have $M = p$, $p_1 = \dots = p_p = 1$, and the third summand in (2) boils down to $\lambda_2 \sum_{m=1}^p \beta_m^2 = \lambda_2 \|\boldsymbol{\beta}\|_2^2$ and, thus, (1) and (3) are equivalent. \square

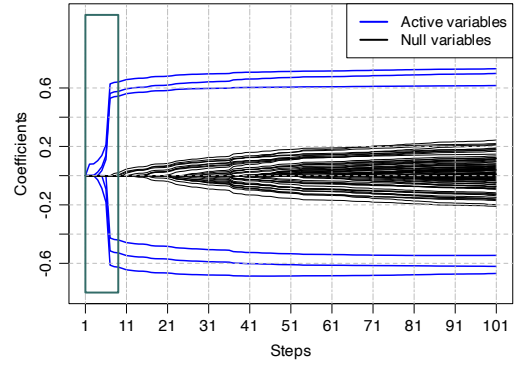
Remark 2. Note that, as desired, the difference of the averaged coefficients of any two variable groups are exactly zero if two variables from different groups are perfectly correlated.

IV. NUMERICAL EXPERIMENTS

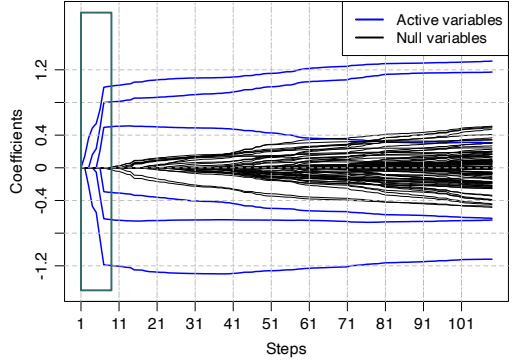
In this section, we evaluate the grouping effect of the EN and the proposed IEN and their relative computation times when incorporated into the *T-Rex* framework.

A. Grouping Effect and Solution Path

To compare the solution paths of the *elastic net* and the proposed *informed elastic net*, we first generate a setting with $p = 100$ and 6 active standard normal variables that are split into two independent groups of highly correlated variables \mathcal{G}_1 and \mathcal{G}_2 (i.e., any pair of the three variables in one group has a correlation of 0.75). The remaining 94 null variables are sampled independently from the standard normal distribution. The coefficient vector $\boldsymbol{\beta} = [\beta_1 \dots \beta_p]^\top$ of the variables is chosen as follows: $\beta_j = 1$ for $j \in \mathcal{G}_1$, $\beta_j = -1$ for $j \in \mathcal{G}_2$ and $\beta_j = 0$ otherwise. The response variable \mathbf{y} is generated from the linear regression model $\mathbf{y} = \mathbf{X}\boldsymbol{\beta} + \boldsymbol{\epsilon}$, where $\boldsymbol{\epsilon} \sim \mathcal{N}(\mathbf{0}, \sigma^2 \mathbf{I})$ is the noise vector. In order to make the grouping effect and the distinction between nulls and active variables visually noticeable, we generated $n = 150$ samples and set the noise variance σ^2 such that the signal-to-noise-ratio $\text{SNR} := \text{Var}(\mathbf{X}\boldsymbol{\beta}) / \text{Var}(\boldsymbol{\epsilon}) = 3$. To obtain the binary support vectors that are required for the data augmentation presented in Theorem 1, we use single-linkage hierarchical clustering with the pairwise correlations between variables as distance measures and cut the resulting dendrogram at the maximum height that satisfies the conservative condition that there exist



(a) Elastic net (EN) solution path.



(b) Proposed: *Informed elastic net* (IEN) solution path.

Figure 2: Solution paths of the (a) EN [15] and (b) IEN.

no two variables from different clusters with a correlation higher than 0.2.

In Figure 2, it can be observed that the EN and the IEN both exhibit the grouping effect in the sense that the coefficients of the two groups of highly correlated active variables are increased in a correlated fashion. We also observe that the grouping effect of the proposed IEN is slightly weaker than that of the EN. However, since we use the IEN as the base selector within the *T-Rex* framework, which terminates the solution paths of all random experiments early, we are primarily interested in the early steps, where a sufficient grouping is observed for both methods, as illustrated in the boxed regions of Figure 2.

B. Relative Computation Time

We compare the relative computation times of one random experiment of

- 1) the original *T-Rex* selector with the *LARS* algorithm as the base selector,
- 2) the *T-Rex+GVS* selector with the EN base selector, and
- 3) the *T-Rex+GVS* selector with the IEN as the base selector

in a setting that is as described in Section IV-A, except that we fix the number of samples to $n = 50$, set the correlation cutoff of the dendrogram to 0.5 and increase p from 100 to 5,000. The computation times are averaged over 50 Monte Carlo replications. In Figure 3, we see that with growing number of variables p , the relative computation time of the *T-Rex+GVS* selector with the proposed IEN as the base selector decreases significantly. In particular, the savings in computation time start to manifest in larger settings with $p \geq 500$ variables, where the EN always needs to augment \mathbf{X} with p (i.e., number of variables) rows, while the IEN only requires augmenting \mathbf{X} with M (i.e., number of groups) rows, where $M \ll p$.

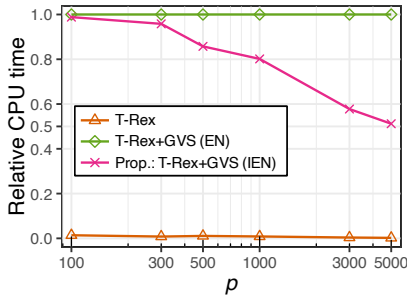


Figure 3: Relative computation times of one random experiment with $L = p$ and $T = 1$ of the T -Rex, T -Rex+GVS (EN), and the proposed T -Rex+GVS (IEN).

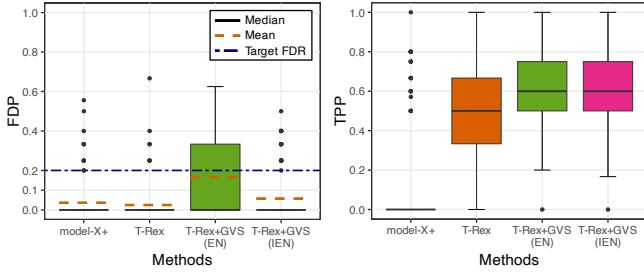


Figure 4: FDP and TPP performances in the simulated GWAS.

V. SIMULATED GWAS

This section presents the results of a GWAS simulation study for which we generate 100 data sets that each contain 500 cases and 200 controls using the software HAPGEN2 [21]. That is, we input real world haplotypes from the HapMap 3 project [22] into HAPGEN2 and the software generates 100 predictor matrices that each contain 1,000 SNPs as columns. The phenotype vector \mathbf{y} contains ones for cases and zeros for controls. For each data set, we generate 10 true active SNPs, while the remaining ones are nulls. The standard preprocessing of genomics data and the evaluation of the results is carried out as described in [14]. As suggested in [11], we run $K = 20$ random experiments for the T -Rex methods.

Figure 4 presents the box plots of the false discovery proportion (FDP) and the true positive proportion (TPP) and the means of the FDP, which are estimates of the FDR, since the FDR is defined as the expectation of the FDP. First, we observe that all methods control the FDR. The median TPP of the benchmark *model-X* knockoff method is zero. The existing T -Rex+GVS (EN) selector shows a significant improvement in TPP compared to the original T -Rex selector. As desired, the significant increase in TPP is also achieved by the proposed T -Rex+GVS (IEN) selector, while the FDP is much lower compared to that of the T -Rex+GVS (EN) selector. Thus, in this GWAS use-case, the proposed T -Rex+GVS (IEN) selector dominates the existing T -Rex+GVS (EN) selector, while exhibiting a much lower computation time, especially in large-scale high-dimensional settings (see Figure 3).

VI. CONCLUSION

We have proposed the *informed elastic net (IEN)*, a fast grouped variable selection method for high-dimensional settings. We incorporated it into the T -Rex framework and showed that it has a significantly reduced computation time in large-scale high-dimensional settings and a better performance in a simulated GWAS compared to the T -Rex+GVS (EN) [14].

APPENDIX

Proof of Theorem 1. First, we rewrite (5) as follows:

$$\mathcal{L}_{\text{IEN}} = (\mathbf{y}'^\top \mathbf{y}' - 2\boldsymbol{\beta}^\top \mathbf{X}'^\top \mathbf{y}' + \boldsymbol{\beta}^\top \mathbf{X}'^\top \mathbf{X}' \boldsymbol{\beta}) + \lambda_1 \|\boldsymbol{\beta}\|_1. \quad (6)$$

Second, note that $\mathbf{X}'^\top \mathbf{X}' = \mathbf{X}^\top \mathbf{X} + \lambda_2 \sum_{m=1}^M \frac{\mathbf{1}_m \mathbf{1}_m^\top}{p_m}$. Then, plugging (4) into (6) yields

$$\begin{aligned} \mathcal{L}_{\text{IEN}} &= \left[\mathbf{y}^\top \mathbf{y} - 2\boldsymbol{\beta}^\top \mathbf{X}^\top \mathbf{y} \right. \\ &\quad \left. + \boldsymbol{\beta}^\top \left(\mathbf{X}^\top \mathbf{X} + \lambda_2 \sum_{m=1}^M \frac{\mathbf{1}_m \mathbf{1}_m^\top}{p_m} \right) \boldsymbol{\beta} \right] + \lambda_1 \|\boldsymbol{\beta}\|_1 \\ &= \mathbf{y}^\top \mathbf{y} - 2\boldsymbol{\beta}^\top \mathbf{X}^\top \mathbf{y} + \boldsymbol{\beta}^\top \mathbf{X}^\top \mathbf{X} \boldsymbol{\beta} \\ &\quad + \lambda_2 \sum_{m=1}^M \frac{\boldsymbol{\beta}^\top \mathbf{1}_m \mathbf{1}_m^\top \boldsymbol{\beta}}{p_m} + \lambda_1 \|\boldsymbol{\beta}\|_1 \\ &= \|\mathbf{y} - \mathbf{X} \boldsymbol{\beta}\|_2^2 + \lambda_1 \|\boldsymbol{\beta}\|_1 + \lambda_2 \sum_{m=1}^M \frac{(\mathbf{1}_m^\top \boldsymbol{\beta})^2}{p_m}. \quad \square \end{aligned}$$

Proof of Theorem 2. Define $\hat{\mathbf{r}} := \mathbf{y} - \mathbf{X} \hat{\boldsymbol{\beta}}$. Taking the first derivative of (2) and setting it equal to zero, we obtain

$$\begin{aligned} \frac{\partial \mathcal{L}_{\text{IEN}}(\boldsymbol{\beta})}{\partial \boldsymbol{\beta}} \Big|_{\boldsymbol{\beta}=\hat{\boldsymbol{\beta}}} &= -2\mathbf{X}^\top \hat{\mathbf{r}} + \lambda_1 \frac{\partial \|\boldsymbol{\beta}\|_1}{\partial \boldsymbol{\beta}} \Big|_{\boldsymbol{\beta}=\hat{\boldsymbol{\beta}}} + 2\lambda_2 \sum_{m=1}^M \frac{\mathbf{1}_m \mathbf{1}_m^\top \hat{\boldsymbol{\beta}}}{p_m} \stackrel{!}{=} \mathbf{0}. \quad (7) \end{aligned}$$

The j th and j' th equation of the system of equations in (7) are:

$$-2\mathbf{x}_j^\top \hat{\mathbf{r}} + \lambda_1 \text{sign}(\hat{\beta}_j) + 2\lambda_2 \frac{\mathbf{1}_1^\top \hat{\boldsymbol{\beta}}}{p_1} = 0, \quad (8)$$

$$-2\mathbf{x}_{j'}^\top \hat{\mathbf{r}} + \lambda_1 \text{sign}(\hat{\beta}_{j'}) + 2\lambda_2 \frac{\mathbf{1}_2^\top \hat{\boldsymbol{\beta}}}{p_2} = 0. \quad (9)$$

Subtracting (9) from (8) and noting that $\text{sign}(\hat{\beta}_j) = \text{sign}(\hat{\beta}_{j'})$:

$$2(\mathbf{x}_{j'}^\top - \mathbf{x}_j^\top) \hat{\mathbf{r}} + 2\lambda_2 \left(\frac{\mathbf{1}_1^\top \hat{\boldsymbol{\beta}}}{p_1} - \frac{\mathbf{1}_2^\top \hat{\boldsymbol{\beta}}}{p_2} \right) = 0. \quad (10)$$

Using (10), we obtain

$$\begin{aligned} \frac{1}{\|\mathbf{y}\|_2} \left| \frac{\mathbf{1}_1^\top \hat{\boldsymbol{\beta}}}{p_1} - \frac{\mathbf{1}_2^\top \hat{\boldsymbol{\beta}}}{p_2} \right| &= \frac{1}{\lambda_2 \|\mathbf{y}\|_2} |(\mathbf{x}_j^\top - \mathbf{x}_{j'}^\top) \hat{\mathbf{r}}| \\ &\leq \frac{1}{\lambda_2} \|\mathbf{x}_j - \mathbf{x}_{j'}\|_2 \frac{\|\hat{\mathbf{r}}\|_2}{\|\mathbf{y}\|_2} = \frac{1}{\lambda_2} \sqrt{2(1 - \rho_{j,j'})} \frac{\|\hat{\mathbf{r}}\|_2}{\|\mathbf{y}\|_2} \\ &\leq \frac{1}{\lambda_2} \sqrt{2(1 - \rho_{j,j'})}, \quad (11) \end{aligned}$$

where the inequality and the equation in the second line follow from the Cauchy-Schwarz inequality and from $\|\mathbf{x}_j - \mathbf{x}_{j'}\|_2 = \sqrt{\|\mathbf{x}_j\|_2^2 + \|\mathbf{x}_{j'}\|_2^2 - 2\mathbf{x}_j^\top \mathbf{x}_{j'}} = \sqrt{1 + 1 - 2\rho_{j,j'}}$, respectively. The last line follows from the fact that $\hat{\boldsymbol{\beta}}$ is the minimizer of (2) and, therefore, $\mathcal{L}(\hat{\boldsymbol{\beta}}) \leq \mathcal{L}(\mathbf{0}) \Leftrightarrow \|\hat{\mathbf{r}}\|_2^2 + \lambda_1 \|\hat{\boldsymbol{\beta}}\|_1 + \lambda_2 \sum_{m=1}^M \frac{(\mathbf{1}_m^\top \hat{\boldsymbol{\beta}})^2}{p_m} \leq \|\mathbf{y}\|_2^2 \Rightarrow \|\hat{\mathbf{r}}\|_2 \leq \|\mathbf{y}\|_2$. Since the inequality in (11) holds for all $j \in \mathcal{G}_1$ and $j' \in \mathcal{G}_2$, the smallest upper bound is given by the largest $\rho_{j,j'}$, i.e.,

$$\frac{1}{\|\mathbf{y}\|_2} \left| \frac{\mathbf{1}_1^\top \hat{\boldsymbol{\beta}}}{p_1} - \frac{\mathbf{1}_2^\top \hat{\boldsymbol{\beta}}}{p_2} \right| \leq \frac{1}{\lambda_2} \sqrt{2 \left(1 - \max_{j \in \mathcal{G}_1, j' \in \mathcal{G}_2} \{\rho_{j,j'}\} \right)}. \quad \square$$

REFERENCES

- [1] A. Buniello, J. A. L. MacArthur, M. Cerezo, L. W. Harris, J. Hayhurst, C. Malangone, A. McMahon, J. Morales, E. Mountjoy, E. Sollis *et al.*, “The NHGRI-EBI GWAS Catalog of published genome-wide association studies, targeted arrays and summary statistics 2019,” *Nucleic Acids Res.*, vol. 47, no. D1, pp. D1005–D1012, 2019.
- [2] Z. Tan, Y. C. Eldar, and A. Nehorai, “Direction of arrival estimation using co-prime arrays: A super resolution viewpoint,” *IEEE Trans. Signal Process.*, vol. 62, no. 21, pp. 5565–5576, 2014.
- [3] K. Benidis, Y. Feng, and D. P. Palomar, “Sparse portfolios for high-dimensional financial index tracking,” *IEEE Trans. Signal Process.*, vol. 66, no. 1, pp. 155–170, 2017.
- [4] D. E. Reich, M. Cargill, S. Bolk, J. Ireland, P. C. Sabeti, D. J. Richter, T. Lavery, R. Kouyoumjian, S. F. Farhadian, R. Ward *et al.*, “Linkage disequilibrium in the human genome,” *Nature*, vol. 411, no. 6834, pp. 199–204, 2001.
- [5] T.-J. Shan, M. Wax, and T. Kailath, “On spatial smoothing for direction-of-arrival estimation of coherent signals,” *IEEE Trans. Acoust., Speech, Signal Process.*, vol. 33, no. 4, pp. 806–811, 1985.
- [6] R. N. Mantegna and H. E. Stanley, *An introduction to econophysics: Correlations and complexity in finance*. Cambridge Univ. Press, 1999.
- [7] Y. Benjamini and Y. Hochberg, “Controlling the false discovery rate: a practical and powerful approach to multiple testing,” *J. R. Stat. Soc. Ser. B. Stat. Methodol.*, vol. 57, no. 1, pp. 289–300, 1995.
- [8] Y. Benjamini and D. Yekutieli, “The control of the false discovery rate in multiple testing under dependency,” *Ann. Statist.*, vol. 29, no. 4, pp. 1165–1188, 2001.
- [9] R. F. Barber and E. J. Candès, “Controlling the false discovery rate via knockoffs,” *Ann. Statist.*, vol. 43, no. 5, pp. 2055–2085, 2015.
- [10] R. Dai and R. Barber, “The knockoff filter for FDR control in group-sparse and multitask regression,” in *33rd Int. Conf. Mach. Learn. (ICML)*, 2016, pp. 1851–1859.
- [11] J. Machkour, M. Muma, and D. P. Palomar, “The terminating-random experiments selector: Fast high-dimensional variable selection with false discovery rate control,” *arXiv preprint arXiv:2110.06048*, 2022. [Online]. Available: <https://arxiv.org/abs/2110.06048>
- [12] E. J. Candès, Y. Fan, L. Janson, and J. Lv, “Panning for gold: ‘model-X’ knockoffs for high dimensional controlled variable selection,” *J. R. Stat. Soc. Ser. B. Stat. Methodol.*, vol. 80, no. 3, pp. 551–577, 2018.
- [13] J. Machkour, M. Muma, and D. P. Palomar, “False discovery rate control for fast screening of large-scale genomics biobanks,” in *Proc. 22nd IEEE Statist. Signal Process. Workshop (SSP)*, 2023, pp. 666–670.
- [14] —, “False discovery rate control for grouped variable selection in high-dimensional linear models using the T-Knock filter,” in *30th Eur. Signal Process. Conf. (EUSIPCO)*, 2022, pp. 892–896.
- [15] H. Zou and T. Hastie, “Regularization and variable selection via the elastic net,” *J. R. Stat. Soc. Ser. B. Stat. Methodol.*, vol. 67, no. 2, pp. 301–320, 2005.
- [16] B. Efron, T. Hastie, I. Johnstone, and R. Tibshirani, “Least angle regression,” *Ann. Statist.*, vol. 32, no. 2, pp. 407–499, 2004.
- [17] J. Machkour, S. Tien, D. P. Palomar, and M. Muma, *TRexSelector: T-Rex Selector: High-Dimensional Variable Selection & FDR Control*, 2022, R package version 0.0.1. [Online]. Available: <https://CRAN.R-project.org/package=TRexSelector>
- [18] R. Tibshirani, “Regression shrinkage and selection via the lasso,” *J. R. Stat. Soc. Ser. B. Stat. Methodol.*, vol. 58, no. 1, pp. 267–288, 1996.
- [19] F. Murtagh and P. Contreras, “Algorithms for hierarchical clustering: an overview,” *Wiley Interdiscip. Rev. Data Min. Knowl. Discov.*, vol. 2, no. 1, pp. 86–97, 2012.
- [20] M. Yuan and Y. Lin, “Model selection and estimation in regression with grouped variables,” *J. R. Stat. Soc. Ser. B. Stat. Methodol.*, vol. 68, no. 1, pp. 49–67, 2006.
- [21] Z. Su, J. Marchini, and P. Donnelly, “HAPGEN2: simulation of multiple disease SNPs,” *Bioinformatics*, vol. 27, no. 16, pp. 2304–2305, 2011.
- [22] The International HapMap 3 Consortium, “Integrating common and rare genetic variation in diverse human populations,” *Nature*, vol. 467, no. 7311, pp. 52–58, 2010.